

Magneto-Optical Traps for Cold Atomic Gravimetry: Research Status and Development Trends

Rui Xu, An Li *, Dongyi Li and Jiujiang Yan

College of Electrical Engineering, Naval University of Engineering, Wuhan 430033, China

* Correspondence: lian196101@126.com

Abstract: The cold atomic gravimeter (CAG) has the advantage of high measurement accuracy and does not need to be calibrated on a regular basis. To achieve cold atom interference, it is first necessary to cool and trap the atoms by magneto-optical trap (MOT). However, there are many types of MOTs, and their trapping and cooling results directly affect the atomic interference, and thus, the measurement accuracy of a CAG. MOTs should be designed or selected correctly for different application needs. This paper reviews the research history of MOTs and analyzes their structure and principles. The current status of applications of different types of MOTs is highlighted. Their advantages and disadvantages are summarized, and perspectives for the development of MOTs for cold atomic gravimetry are presented.

Keywords: cold atom gravimeter; magneto-optical trap; Doppler cooling; atom trapping; atom funnel

1. Introduction

Gravity sensors can be used to detect any underground object that creates a difference in mass. This can help analyze geological formations and locate buried infrastructure. While technologies such as ground-penetrating radar can do this, they must send a signal underground and they are active technologies, which limits their measurement depth. The advantage of gravity measurement is that it is passive and does not require a signal to be sent underground, so the ground does not attenuate the signal. As long as the signal generated by the object at the surface is strong enough, it can be detected. In theory, there is no limit to the measurement depth.

Laser interferometric gravimeters measure gravity using the free fall of an angular cone; their measurement accuracy is restricted by the optical diffraction limit. Cold atomic gravimeters (CAGs) using the interference of cold atoms, without mechanical wear and tear, do not require periodic calibration. The measurement speed is faster, and long-term continuous measurements can be achieved. The long-term precision of the atom gravimeters in a seismic station is better than $2 \mu\text{Gal}$ ($1 \mu\text{Gal} = 10^{-8} \text{m/s}^2$), which is comparable to the best classical gravimeter FG-5(X). The measurement sensitivity has already reached $38 \mu\text{Gal}/\sqrt{\text{Hz}}$ with the potential for improvement [1]. CAGs are widely used for precise measurement due to their high sensitivity and accuracy. They have made outstanding contributions to geological monitoring [2,3], metrological studies [4,5], and fundamental physics research [6,7] in recent years. They have also improved the accuracy of inertial navigation [8,9]. High-precision gravity measurements are required for underwater gravity navigation. In the underwater navigation of submarines, conventional sonar technology cannot receive a signal in deep water. High-precision gravity maps of the seafloor can be used to help the submarine quickly locate and avoid obstacles on the seafloor.

CAG uses cold atoms as measuring media. During the operation of a CAG, atoms are first cooled and trapped under the control of a magnetic and optical field. Then, the magnetic field is turned off and the trapped cold atomic cluster is allowed to fall freely or thrown vertically. The atoms are prepared to the magnetic field's insensitive state $m_F = 0$.



Citation: Xu, R.; Li, A.; Li, D.; Yan, J. Magneto-Optical Traps for Cold Atomic Gravimetry: Research Status and Development Trends. *Appl. Sci.* **2023**, *13*, 6076. <https://doi.org/10.3390/app13106076>

Academic Editor: Galina Nemova

Received: 16 April 2023

Revised: 10 May 2023

Accepted: 12 May 2023

Published: 15 May 2023



Copyright: © 2023 by the authors. Licensee MDPI, Basel, Switzerland. This article is an open access article distributed under the terms and conditions of the Creative Commons Attribution (CC BY) license (<https://creativecommons.org/licenses/by/4.0/>).

At the first moment, $t = 0$, a $\pi/2$ pulse is applied to the atomic cluster, which is distributed from the ground state $|a, \mathbf{P}\rangle$ to the excited states of $|a, \mathbf{P}\rangle$ and $|b, \mathbf{P} + \hbar\mathbf{k}_{\text{eff}}\rangle$. The two clusters of split atoms have different momentums and evolve freely along different paths. The phase of the laser is transferred to the atoms. At time $t = T$, a π pulse is applied to the atomic cluster, and the atomic cluster on the two states reverses, as shown in Figure 1. At time $t = 2T$, another $\pi/2$ pulse is applied to the atomic cluster. A beam combination occurs to the atomic wave packet; interference happens due to the presence of phase difference.

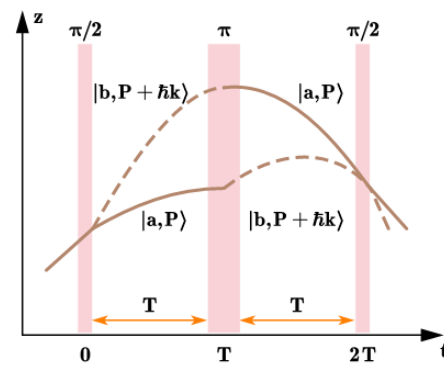


Figure 1. Schematic diagram of the working principle of the pulsed Raman atomic interferometer in the gravitational field.

The fluorescence signal of atoms is probed to calculate the probability of distribution of the atom at different energy levels. The probability that atoms in the ground state energy level is $P = (1 - \cos \Delta\phi)/2$. The phase difference $\Delta\Phi$ arises from the phase transfer of photons and atoms $\Delta\Phi_{\text{laser}}$ and the difference in the path of the free evolution of the atoms $\Delta\Phi_{\text{evolution}}$ under the effect of gravity. The phase difference satisfies the equation $\Delta\Phi = (k_{\text{eff}} g - 2\pi\alpha)T^2$. k_{eff} is the effective laser wave vector. T is the time interval between two adjacent Raman laser pulse beams. α is the scanning chirp rate. The frequency of Raman leap is chirped and scanned to compensate for the Doppler shift. When the Doppler shift is compensated, the cold atoms resonate with the Raman laser. When $k_{\text{eff}} g - 2\pi\alpha = 0$, changing the pulse interval T , all cosine curves will intersect at a point. The value of gravitational acceleration can be calculated using the chirp rate α at that point [10].

Quantum projection noise (QPN) is one of the main sources of noise in atomic interferometric gravimetric experiments. QPN is determined by the number of atoms N involved in the interference, and it is proportional to $1/\sqrt{N}$. The accuracy and sensitivity of the CAG measurement increases with the number of atoms involved in the interference [11]. The cooling and confinement of the atoms during this process is particularly important and directly affects the subsequent interference results in the vacuum cavity. However, there are few papers devoted to the structural characteristics and trends of magneto-optical traps. Atoms move very fast at room temperature, and their low density does not make them easy to manipulate. The lower the temperature, the slower the atoms move. The temperature of the atomic cluster should be reduced to the order of μK for interference to occur. At such a low temperature, there will be more atoms trapped. The cooling and trapping of the atoms is usually achieved by magneto-optical traps.

In 1865, the British physicist James Maxwell proved that photons can act mechanically [12]. With the invention of lasers, the idea of the manipulation of atoms by means of lasers was born. The concept of atomic traps was first introduced in 1978 by Letokhov et al. [13] at the Institute of Spectroscopy of the USSR Academy of Sciences. They used the scattering and dipole forces of the laser to control the motion of atoms in the optical field. When a cluster of atoms is irradiated with a large detuned laser standing wave field, the atoms are pushed by dipole forces to the lowest potential energy wave vents and nodes, forming atom traps. However, since only one-dimensional standing waves were analyzed and the number of trapped atoms was small, a potential trap was needed

to hold the atoms at a stable equilibrium point in space. This was followed in 1979 by Ashkin's proposal to construct an atomic trap using the combination of the dipole and scattering forces [14]. Atoms are causally trapped near the center of the intersection of the two laser beams by using two large detuned Gaussian laser beams propagating in opposite directions. However, this idea has not been realized experimentally. With further research on MOTs, in 1983, Dalibard and Cohen-Tannoudji et al. proposed a scheme to overcome the heating effect of atoms by allowing the trapped and cooled laser beams to work in a time-sharing manner to confine them, but it was also not realized experimentally [15].

Summarizing the problems encountered in trapping cold atoms, Gordon et al. [16] proved the Earnshaw theorem for optical radiation in 1983, showing that the scattering force alone cannot trap an atom at an equilibrium point in free space, leading to the conclusion that the gradient force or dipole force is essential for any successful optical trapping. Inspired by this theorem, in 1984, Ashkin [17] proposed to alternate the direction of the two laser beams and use the alternating electric field instead of the electrostatic field to form a stable atom trap using only pure scattering forces, and he successfully trapped oil particles in the experiment, breaking the limits of Earnshaw's theorem for optical radiation. In 1986, a single-beam Gaussian laser was first used to realize a laser dipole force trap in sodium atomic vapor by Steven Chu. They first cooled the atoms into optical molasses, then irradiated the optical molasses with a Gaussian beam. A dipole force trap was buried in an optical molasses with a temperature of about 240 μK and a diameter of about 1 cm. They finally achieved the trapping of atoms in a wide range of laser power and frequency detuning [18].

Building on the previous methods, in 1986, Pritchard et al. proposed three ways to use external fields to break the limits of the optical Earnshaw theorem [19]: (1) Using an external field, such as a magnetic field, to make the transition frequency of the atom vary with space; (2) Using an external field to make the atomic orientation vary with space; (3) Using optical pumping to change the atomic state. They found that the atomic potential trap obtained by this method would have a much greater trap depth than the dipole force trap, and it can trap more atoms and at a lower temperature. Inspired by this idea, MOT was created. Dalibard first proposed the construction of atomic traps by combining an inhomogeneous static magnetic field and optical pressure. This idea was soon taken up and implemented jointly by Steven Chu's group at Bell Labs and Pritchard's group at MIT in 1987 [20]. They modified the device that produces the optical molasses. Six quarter-wave plates were installed to produce circularly polarized laser beams. A pair of coils with opposite currents was used to generate the desired quadrupole magnetic field. A magnetic field gradient was used to tune the atomic resonance so that the radiation pressure provided both cooling and damping forces. In this way, 10^7 atoms were trapped in two minutes, and the atomic density reached $2 \times 10^{11} / \text{cm}^3$ at a temperature of 600 μK . They called the atomic trap a MOT. In 1988, Letokhov et al. [21] first proposed the use of six orthogonal standing wave laser beams to cool trapped atoms in their overlapping region; they achieved the trapping of atoms in the standing wave laser field. They found that in the standing wave field, cold atoms could be stored for a long time in the cross-sectional region of laser beam under high laser intensity and low-pressure conditions. Since then, MOTs have been widely studied and applied worldwide.

The other sections of this paper are organized as follows: the second section gives an introduction to the working principles of a MOT; the third section presents the research history on and structure of MOTs. This section contains a review of applications for different types of MOTs, the fourth section gives a summary of and discussion on the prospective development of MOTs for cold atomic gravimetry.

2. Working Principle of the MOT

2.1. Cooling of the Atoms

A moving atom is subject to the Doppler effect in laser beams. If the atom moves in an opposite direction to that of the beam propagation, the magnitude of this motion is

kv ; v is the projection of the atomic velocity in the direction of beam propagation. $\hbar k$ is the momentum of the photon. F_1 is the force on the atom against the direction of laser propagation; F_2 is the force on the atom with the same direction of laser propagation [22,23]:

$$\begin{aligned} F_1 &= -\hbar k \frac{\Gamma}{2} \frac{I/I_{sat}}{4(\delta+kv)^2/\Gamma^2+(1+2I/I_{sat})} \\ F_2 &= +\hbar k \frac{\Gamma}{2} \frac{I/I_{sat}}{4(\delta-kv)^2/\Gamma^2+(1+2I/I_{sat})} \end{aligned} \tag{1}$$

As can be seen in the above equation, the laser has a decelerating effect on moving atoms only when the direction of the atomic motion goes against the direction of the beam, and the laser frequency is tuned below the atomic resonance frequency. In one-dimensional Doppler cooling, the cooling force is generally achieved by using two separate laser beams. As shown in Figure 1, each beam of intensity I exerts a force on the atom, and the combined force on the atom is F .

$$F = F_1 + F_2 \tag{2}$$

I is laser intensity; I_{sat} is saturation laser intensity; Γ is the natural line width, and δ is the detuning. Figure 2 shows that near $v = 0$, the combined force on the atom varies linearly with velocity. When the direction of the incident laser is the same as the direction of the motion of the atom with velocity magnitude v , the laser detuning felt by the atom is $\delta + kv$, and when the direction of the incident laser beam goes against the direction of motion of the atom, the laser detuning felt by the atom is $\delta - kv$. Therefore, if the atom propagates in the opposite direction to the laser beam, the atom can absorb photons into the excited state, but the direction of the radiation pressure of the laser received at this time is goes against the direction of the atom's motion, thus achieving the effect of decelerating the atom and realizing the Doppler cooling process. The best cooling effect can be obtained by choosing an appropriate amount of optical detuning ($\pm\delta$) so that the combined force of the radiation pressure on the atom is maximized.

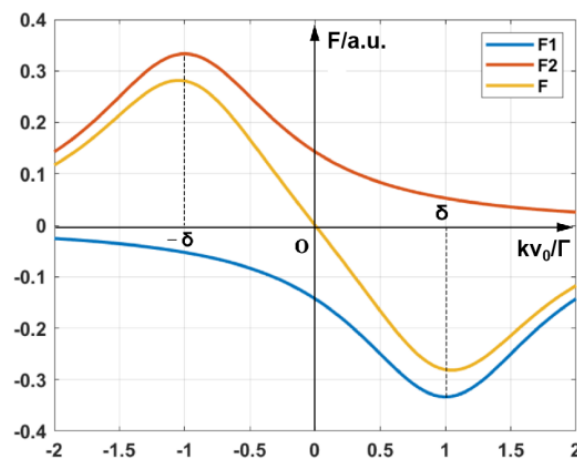


Figure 2. The scattering force exerted on an atom by two laser beams with a detuning of δ .

In 1987, Steven Chu and Hall continued to apply cooling laser beam to keep the atoms in the optical molasses after turning off the gradient magnetic field, and found that the temperature of the atoms obtained from the final confinement was well below the Doppler cooling limit; the result suggested the existence of a polarization gradient cooling mechanism in MOT [24,25]. Considering the multi-energy level structure of the atoms, the final cooling temperature is proportional to the optical shift of the ground state energy level. Increasing laser detuning or decreasing laser power can reduce the optical shift to further decrease the cooling temperature, resulting in sub-Doppler cooling [26].

2.2. Trapping of the Atoms

The trapping of atoms in MOTs is mainly based on the scattering force of the laser. The gradient magnetic field generated by a pair of inverse Helmholtz coils causes the magnitude and direction of the pressure of laser radiation on the atoms to vary with the spatial position, while providing atoms in the coil region with a scattering force directed toward the center of the magnetic field. As shown in Figure 3a, δ is laser detuning, δ_+ is positive detuning, and δ_- is negative detuning. Taking the one-dimensional case as an example, consider a two-energy atom with only one energy level in the ground state(g) and total angular momentum $J = 0$. There is no Zeeman shift or splitting in the magnetic field. The excited state(e) $J = 1$ splits into three magneton energy levels $m_J = -1, 0, 1$ due to the Zeeman effect in a weak magnetic field generated by a pair of inverse Helmholtz coils. The leap of this atom is as follows: $J = 0 \rightarrow J = 1$. The magnetic field is zero at the origin of the coordinates and increases linearly along the axes. The energy level produces a Zeeman shift; the ground state remains unchanged. The excited $m_J = 1$ sublevel increases linearly along the coordinate axis and decreases linearly along the negative direction. The opposite is true for the $m_J = -1$ sublevel. There is no change in the $m = 0$ sublevel. A pair of opposite laser beams of the same intensity, tuned to their frequencies, are negatively detuned for the atoms at $z = 0$, while the directions of polarization are σ_+ and σ_- . The laser frequency at $Z > 0$ is closer to the leap frequency of $m_J = 0 \rightarrow m_J = -1$ due to the Doppler effect, and will absorb more σ_- photons. The atom is subjected to a restoring force pointing to the origin of the coordinates. Similarly, the laser frequency at $Z < 0$ is closer to the leap frequency of $m_J = 0 \rightarrow m_J = 1$ due to the Doppler effect and will absorb more σ_+ photons. In summary, atoms that deviate from the center of the magnetic field are subjected to a scattering force directed toward the center, which traps the atoms in the center of the field. The actual alkali metal atoms also have a hyperfine energy level structure in the ground state, but the principle of cooling and trapping atoms is the same.

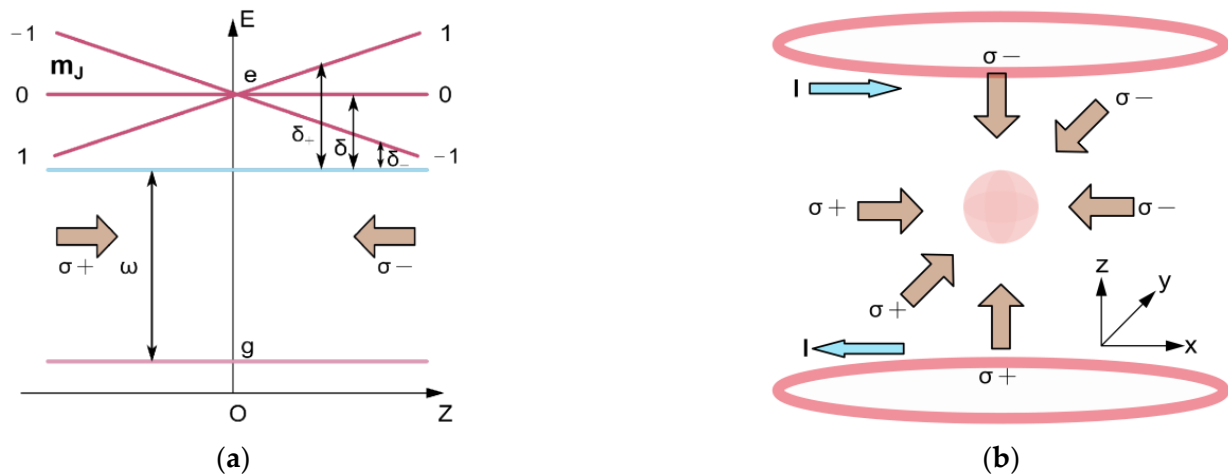


Figure 3. Trapping of cold atoms: (a) is the atomic-level stuffing displacement diagram and (b) is the three-dimensional MOT schematic.

To ensure effective interferometric processes in atomic gravimetry applications, the MOT usually needs to capture cold atoms of order 10^7 , and the atomic temperature needs to be reduced to μk level to achieve good measurement accuracy. The number of cold atoms trapped in MOTs is typically measured by various methods [27], such as fluorescence intensity calculation [28], resonance absorption detection, and fluorescence detection [29,30]. The fluorescence emitted by the atoms is received by a photomultiplier (PMT). Photocurrent signals are converted into voltage signals by the current–voltage conversion circuit and are finally detected. The fluorescence intensity represents the number of atoms resonantly absorbed by the laser at that frequency. The time-of-flight method [31,32] is commonly used to measure the temperature of cold atomic clusters. The principle of the time-of-flight

method is to measure the thermal motion of the atoms. The motion of the atoms is closely related to their temperature. After the magnetic field is turned off, the atoms fall freely under the influence of gravity. The cooling temperature as well as the initial velocity distribution can be determined by recording the time they need to reach the detection area. The measurement principle is shown in Figure 4.

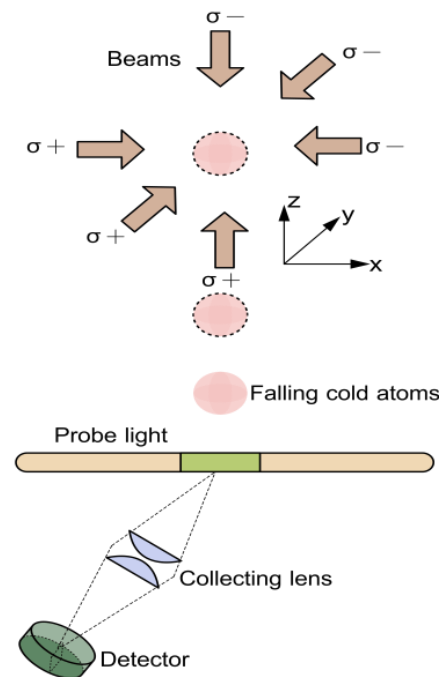


Figure 4. Schematic of the time-of-flight method for cold atom temperature measurement.

3. Classification and Application of MOTs

According to the atom trapping principle, MOTs can be classified into dark magnetic traps [33], spin-polarized magnetic traps [34], pyramidal MOTs [35,36], conical and axial-conical MOTs [37,38] and so on. According to the structure of MOTs, they are mainly divided into two-dimensional MOTs [39–43] and three-dimensional MOTs [44].

3.1. Application of Conventional Six-Beam MOT

The initial six-beam MOT is realized by six red-detuned polarized laser beams and a gradient magnetic field. A three-dimensional standing wave optical field was created by three pairs of orthogonal laser beams, which converted from a linearly polarized laser to a circularly polarized laser after passing through six quarter-wave plates. A pair of inverse Helmholtz coils, spaced at the coil radius, provided a linear gradient magnetic field to overcome the limitations of Earnshaw's optical theorem. The center of the magnetic field coincides with the center of the optical field. The magnitude of the magnetic field is 0 at the center of the field and increases linearly in the x , y , and z directions. The first stable six-beam MOT was achieved in 1990 by Monroe et al. at the American Institute of Astrophysics [45], with a structure similar to that shown in Figure 3b. I is the current in the coil; the arrow direction indicates the current direction. The MOT trapped about 1.8×10^7 atoms with atomic temperatures down to $1.1 \pm 0.2 \mu\text{K}$, the lowest temperature achieved in atomic trap studies at that time. The advantage of the six-beam MOT is that the structure is simple and easy to implement, and the number of captured atoms is relatively stable despite changes in the shape of the atomic clusters. Six-beam MOTs are widely used in CAG because of the high number of cold atoms trapped and the ability to achieve extremely low cooling temperatures.

In 2013, the dynamic measurement of gravity was achieved with the GAIN gravimeter developed by Peter et al. at Humboldt University in Germany, which used a six-beam MOT.

The structure of GAIN is shown in Figure 5. K_1 and K_2 are the wave numbers of the Roman transitions. RF is a radio frequency signal. The temperature of the atomic clusters was $2 \mu\text{k}$, and the number of trapped ^{87}Rb atoms reached 10^9 in 0.6 s. They show the best reported performance of mobile CAG in data, with an accuracy of $3.9 \mu\text{Gal}$ and a short-term noise of $9.6 \mu\text{Gal}/\sqrt{\text{Hz}}$ [46,47].

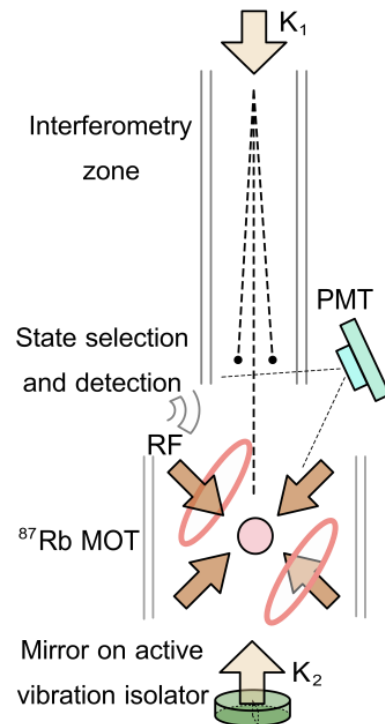


Figure 5. Structure of GAIN gravimeter.

The gravimeter designed by Bidel et al. at the French Aerospace Laboratory used a six-beam MOT to trap about 10^6 atoms in 20 ms; it obtained cold atomic with a temperature of $1.9 \mu\text{k}$. The group successfully completed gravity dynamics measurements at sea in 2018 under linear and circular navigation conditions. Despite rough sea conditions, they obtained precision below 1mGal [48]. Airborne gravity dynamics measurements were completed in Iceland in 2020, with an estimated error between 1.7 and 3.9mGal [49]. In 2021, a six-beam MOT was used in the rubidium atomic absolute gravimeter, which developed by Li et al. This MOT captured about 10^8 atoms with a cooling temperature of $5 \mu\text{k}$ [50].

Six-beam MOTs are widely used in cold atomic gravimetry; they are capable of trapping more than 10^7 atoms with cooling temperatures in the μk range, fully meeting the measurement accuracy requirements of atomic gravimetry.

3.2. Other MOT Attempts

In 1991, Shimizu et al. found that when four of the six laser beams in a MOT are misaligned, the trapping capacity of the MOT increases, while atomic clusters are formed. They proposed and constructed a MOT with less than six laser beams and designed a MOT scheme with four laser beams, as shown in Figure 6. This MOT successfully trapped 4×10^7 atoms of ^{20}Ne [51,52].

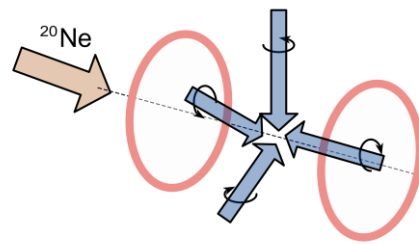


Figure 6. Structure of four-beam MOT.

The advantage of the four-beam MOT is that the laser beam is reflected back along different paths, and the laser beam coming out of the MOT can be used for other purposes. However, due to the difficulty of beam adjustment, the cooling and trapping of atoms is less effective than that of the six-beam MOT; therefore, it is rarely used in cold atomic gravimetry.

In 1998, Arlt and di Stefano attempted to implement a MOT for Cesium atoms using a five-beam configuration, as shown in Figure 7. In this scheme, two laser beams were projected in opposite directions along the axis of the quadrupole trap, with the polarization states of $\sigma+$ and $\sigma-$, respectively. The remaining three laser beams propagate opposite each other at an angle of 120° in the orthogonal plane, and all of them have a polarization state of $\sigma+$. Briefly, di Stefano compared the number and density of atoms trapped in five- and six-beam magneto-optical traps, and showed that the trapped population in the five-beam MOT is 15% smaller than in the six-beam MOT. The atomic densities are of the same order. The lowest temperature achieved with the five-beam MOT is $3.8 \mu\text{K}$, slightly higher than the $2.3 \mu\text{K}$ achieved with the six-beam configuration [53].

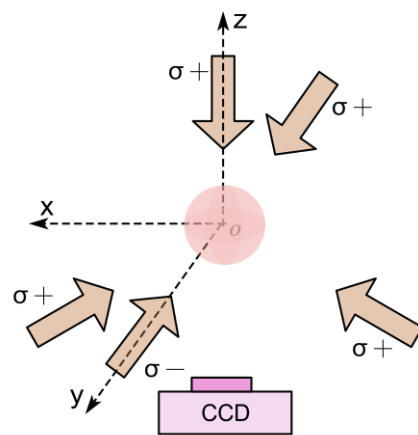


Figure 7. Five-beam MOT schematic.

In summary, the five-beam MOT provides a convenient alternative to the six-beam configuration, with the advantage of capturing more atoms in less time. In Arlt's study, a slower Zeeman coil was used in conjunction with a five-beam MOT. One beam in the horizontal was directed against the atoms as they entered the trapping region. This increased the effective stopping distance of atoms [54].

3.3. Rise of Single Beamed MOTs

To meet the measurement requirements in dynamic field environments, such as ship-board [55,56], airborne [57], and vehicle-mounted [58,59], the miniaturized design of CAG is crucial. The key technologies for miniaturization are the integrated design of a laser system [60–64] and the compact design of the vacuum cavity. The size of a sensor head can be reduced by simplifying the conventional six-beam MOT to a single-beam MOT. The principle is that in the trap region, similar to a six-beam MOT, only a circularly polarized

beam-expanding laser and mirrors [65] are used to form an optical configuration. The mirrors can be pyramidal or axially conical.

In 1996, Lee et al. first proposed this novel and simple design of MOT by using a tetrahedral mirror reflection with only one laser beam, as shown in Figure 8. The number of cold atoms trapped in this MOT at a loading time of 400 ms is about 1.2×10^7 [38]. Lee's study shows that the polarization contamination of the incident circularly polarized laser is less than 1%. The power loss of the laser due to the reflection of the metal mirror is less than 12%, and the reflectivity of the aluminum mirror is greater than 88%. The experimental results indicated that the confinement characteristics of this single-beam MOT are largely unaffected.

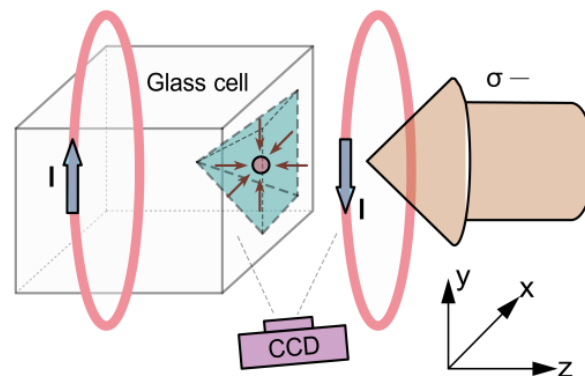


Figure 8. Pyramidal MOT structure.

In 1996, Lu at the University of Colorado at Boulder proposed a slow-velocity intense source with a loading rate of 70% [66]. In 1998, Lee's pyramidal MOT design was adapted into an atomic funnel by Williamson et al. at the University of Wisconsin [67]. A small hole is opened at the top of the pyramidal mirror. A set of 1/4 waveplates and plane mirrors are placed in opposite directions to form two mid-axis directionally opposing laser beams. The feature of this optical configuration is that cold atoms can be pulled out through the small hole, and then a high flux beam of cold atoms can be formed [68,69]. Loading into a second MOT can improve its efficiency. The simple structure and compact design of this single-beam pyramidal funnel gives it an advantage for loading MOTs in ultra-high vacuum environments.

In 2010, Bodart et al. [70] realized a compact cold atom gravimeter scheme that achieves the cooling and trapping of atoms using a hollow pyramidal structure. They demonstrated a relative sensitivity to acceleration of gravity of $17 \mu\text{Gal}$ at one second. The group trapped about 4×10^6 ^{87}Rb atoms in a loading time of 360 ms. After an optical molasses phase of 20 ms, the laser was adiabatically turned off and the atoms were allowed to fall. The temperature of the cold atoms was measured by Raman velocimetry [71] to be $2.5 \mu\text{K}$, which is comparable to the temperature obtained by a six-beam MOT. This was followed in 2013 by the development of the "MiniAtom" transportable atomic gravimeter with a pyramidal MOT, which loads about 10^7 atoms in 400 ms. The long-term stability was in the 10^{-9} range and up to two days of measurements with this type of architecture [72]. The reduction in the beam allows a significant reduction in the size of the sensor head, which can fit into a cylinder 40 cm high and 20 cm in diameter. It saves a lot of space compared to the transportable absolute gravimeter developed by SYRTE with a cylindrical sensor head that is 80 cm high and 50 cm wide [73]. In 2018, the French company Muquans launched a commercial removable absolute gravimeter product. It was based on a hollow pyramidal MOT. This trap was loaded with 10^7 ^{87}Rb atoms in 250 ms at an atomic temperature of $2 \mu\text{K}$. The measurement of the absolute gravitational acceleration has been performed continuously with a long-term stability below $1 \mu\text{Gal}$ [74]. The gravimeter can be used for both continuous observatory measurements and gravity mapping, and can be set up in less

than 20 min. During installation, the operator only needs to adjust the perpendicularity of the sensor head and it is ready for measurement after a 1 h warm-up time.

In 2019, Wu and Müller et al. [75,76] developed a new mobile CAG, which used an inverted MOT with a through-hole pyramidal shape. It was realized to measure the absolute gravity at Berkeley Hills in a field vehicle-mounted environment. A plane mirror was used as a reflector in this MOT, which eliminates the effect of the pyramid top angle defect and the wavefront aberration caused by the pyramid edge on the system. The MOT achieved a loading time of 150 ms to trap about 5×10^7 Cesium atoms. After the magnetic field was turned off, the temperature of the atomic cluster was further cooled to $2 \mu\text{K}$. In laboratory operation, they achieved a sensitivity of $37 \mu\text{Gal}/\sqrt{\text{Hz}}$ and a stability of $2 \mu\text{Gal}$ in half an hour. In the field, the mobility allowed them to measure gravity in the field with a resolution of around $0.5 \text{ mGal}/\sqrt{\text{Hz}}$. This structure is simpler and more efficient than a conventional pyramidal CAG [77]. As key means of miniaturizing CAG, pyramidal MOTs have been widely used.

3.4. Two-Dimensional MOT for Precooling

Inspired by pyramidal atomic funnels, Dieckmann of the Netherlands Institute used a two-dimensional MOT (2D-MOT) in 1998. There was a through-hole in the reflector to obtain a cold atomic beam of 8 m/s from a rubidium vapor chamber. The flux of the cold atomic beam was 9×10^9 atoms/s [78]. The experimental setup is shown in Figure 9. In the figure, I is the current in the coil; the arrow direction indicates the current direction.

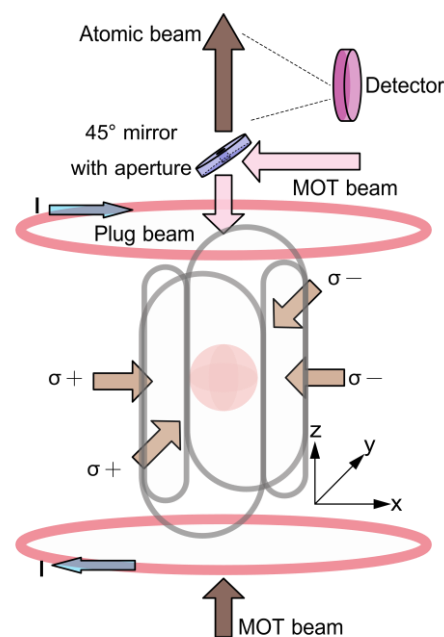


Figure 9. Two-dimensional MOT setup.

In 2019, Zeng et al. used a 2D-MOT to generate cold atomic beams, resulting in a loading rate of 2.8×10^9 atoms/s for a three-dimensional MOT (3D-MOT) [79]. In 2022, Wang et al. designed a CAG for on-board dynamic measurement of absolute gravity in the external field. They used a 2D-MOT pre-cooling, and a six-beam MOT accessed through a differential tube to finally trap about 10^8 atoms in 300 ms with a cooling temperature of $6 \mu\text{K}$ [80]. In 2023, Jin at the Institute of Physics in Heidelberg replaced the conventional Zeeman reducer with a 2D-MOT to produce a high-flux slow atomic beam. This led to a 3.6-fold increase in the loading rate of a 3D-MOT, with a loading rate of 10^8 atoms/s, trapping about 3×10^8 atoms. The cold atom temperature was $15 \mu\text{K}$ [81].

For the pre-cooling of atoms, 2D-MOTs are often used in atomic gravimetry due to their special structure. The cold atomic beam enters a 3D-MOT through a differential tube,

which has the advantage of eliminating background gas interference and improving the loading efficiency of the 3D-MOT [82].

3.5. Extremely Miniaturized MOT Development

In the pursuit of extreme miniaturization of cold atom sensors, the integration of optical elements with atomic chip techniques [83,84] for the detection and quantum coherent operation of cold atoms is being extensively investigated. Similar to the principle of a macroscopic pyramidal MOT, a microscopic pyramidal magneto-optical trap (PMOT) can also be used to cool and trap small arrays of atomic clouds on the chip. Planar diffraction gratings fabricated and integrated by photolithography enabled grating the magneto-optical trap (GMOT) [85], further reducing the size of the cold atom sensor platform. Table 1 shows the research on MOTs on chips that has been created in recent years.

Table 1. Status of research on MOTs on chips.

Year	Institution	Type	Results	Reference
2009	Imperial College London Blackett Laboratory	PMOT	2000 ^{85}Rb atoms at a temperature of 100 μk	Pollock et al. [86,87]
2009	University of Strathclyde	PMOT	1.3×10^6 atoms	Vangeleyn et al. [88]
2013	University of Maryland	PMOT	5×10^5 atoms at a temperature of 10 μk	Lee et al. [89]
2017	University of Strathclyde	GMOT	3×10^6 atoms at a temperature of 3 μk in 10 ms	McGilligan et al. [90]
2019	National Institute of Standards and Technology in Maryland	GMOT	10^{67}Li atoms	Barker et al. [91]
2021	University of Maryland	GMOT	10^7 atoms at a temperature of 146 μk in 0.25s	McGehee et al. [92]
2022	University of Birmingham	PMOT	2.1×10^7 cold atoms	Earl et al. [93]
2022	Sandia National Laboratories	GMOT	0.17 cm^3 atomic cluster at a temperature of 15 μk	Lee et al. [94]
2022	China Academy of Metrology	GMOT	2.8×10^7 ^{87}Rb atoms	Duan et al. [95]
2022	China Academy of Metrology	GMOT	10^6 ^{87}Rb atoms	Duan et al. [96]

In 2021, McGehee et al. [91,92] showed that grating chips are compatible with holes. Future chip-level cold atomic beams can be achieved by introducing holes in the center of the chip. In 2022, Luuk Earl et al. [93] carried a MOT with dimensions of 370 mm \times 350 mm \times 100 mm, a weight of 6.56 kg, and a power of 80 watts on board an unmanned aircraft. Their work paved the way for an unmanned portable cold atom gravimeter. In the same year, the planar inverse Helmholtz coil chip proposed by Duan et al. [96] greatly reduced the power consumption and volume of the GMOT. They pointed towards a new direction of development for integrated cold atom gravimetry and portable precision measurement systems [94]. Combined with techniques such as passive pumping [97], it is possible to develop a cubic centimeter volume cold atom physical package in the future.

Integrated chips designed with the GMOT have been successfully used for fundamental physics research [98,99]. Since the GMOT enables a large optical volume overlap [100], it has been applied in miniaturized cold atom systems for cold atom clocks [101] and slow cold atom beam preparation [102]. It is also widely used in cooling and trapping various

types of atoms, including Rb atoms, Li atoms [103], and Sr atoms [104]. Grating-based 2D-MOTs [105] and a new method for trapping alkaline earth atoms [106] have been realized. Using GMOT can further compress the size of optical components into a portable, packable laser cooling platform [107–109].

Due to their size advantage, PMOT and GMOT are widely used in the research on the integration of cooling platforms. However, the number of atoms available for PMOTs is limited by etching depth and processing techniques. GMOT is also affected by the diffraction efficiency of grating. The performance of GMOT can be further improved by improving diffraction efficiency in the future.

4. Conclusions and Outlook

Cold atom gravimetry is currently an important tool for precision gravity measurements. The interferometric effect of cold atoms directly affects the precision measurement results. The MOT is a key structure for preparing cold atoms, and the number and temperature of the trapped cold atoms directly affect the interference effect. Different types of MOTs have their own advantages and disadvantages, and they should be selected for different uses. Table 2 summarizes the different types of MOTs.

Table 2. Features and applications of different types of MOTs.

Type	Advantages	Disadvantages	Use Cases
Six-beam MOT [44–49]	High number of cold atoms and low temperature.	Large size, complex optical path.	Scientific research institutes, schematical prototypes.
Four-beam MOT [50,51]	Captures more atoms in less time.	Difficult beam adjustment.	Used in conjunction with a slower Zeeman coil for efficient atom trapping.
Five-beam MOT [52,53]	Insensitive to laser beam phase fluctuations.	Low cold atom number.	Removal of the cooled atoms from the cooling beam for other studies.
Single-beam MOT [74–76]	Pre-cooling of atoms, small size for dynamic measurements.	Difficult mirror surface processing.	Field dynamic measurements, used with six-beam to produce cold atomic beams.
2D-MOT [78–80]	Pre-cooling of atoms.	Unsatisfactory cold atom preparation.	Used in conjunction with 3D MOTs to produce cold atomic beams.
PMOT [85–88]	Very compact size.	Etch depth limits the number of cold atoms.	Integrated cold atom sensor.
GMOT [93–95]	Large optical overlap volume, very compact size.	Low grating diffraction efficiency.	Miniaturized cold atom system.

In this paper, the generation and development of MOTs are reviewed. The different types of MOTs are summarized and discussed in terms of structure, principle, and applications. It can help early stage teams in atomic gravimetry and other related fields to quickly understand MOTs. A reference for selecting a suitable MOT is provided. Listed developments and trends can be compared to their MOTs to help determine how to optimize their use. Six-beam MOTs are often chosen by research institutions to meet ultra-high accuracy measurement requirements in station gravimeters and schematical prototypes.

The efficiency of cooling and trapping atoms can be affected by laser intensity, detuning, and magnetic field gradients. There are four ways to improve the loading rate of MOTs, including: (1) Increasing the background atomic density; (2) Effectively increasing the capture beam diameter; (3) Increasing the quadrupole magnetic field gradient; (4) Optimizing the parameters to improve the trapping capacity of the MOT itself. This will further improve the measurement accuracy of CAG.

CAG for commercial and field measurements tends to favor the more compact single-beam MOT. Four- and five-beam MOTs are less commonly used in atomic gravimetry because of their special design and general effectiveness in cooling and trapping atoms. Mostly, 2D-MOTs are used to improve the loading efficiency of 3D-MOTs. Chip MOTs have developed rapidly in recent years, and if processing difficulties can be overcome, CAG packages with cubic centimeter volumes may be realized in the future. With the help of complex mirror processing, the MOT has evolved from being six-beam to being single-beam. The number of lasers and the complexity of the optical path have been reduced by mirror reflection technology. The sensor head is more compact in size, lighter in mass, and consumes less power. It can better meet the requirements of portable and dynamic measurements. With the development of atomic chip techniques, the MOT has been simplified from a three-dimensional structure to a flat structure, further reducing its power consumption and size. Therefore, there are two main directions for future development: (1) Reducing the size of the vacuum chamber as much as possible while retaining the number of trapped atoms. For example, the evolution from a six-beam MOT to single-beam MOT better meets the needs of portable and dynamic measurements; (2) Improving processing accuracy and increasing the number of trapped atoms while maintaining a small size, and combining with the miniaturization of other hardware parts of the atomic gravimeter to achieve chip-level CAG.

Author Contributions: R.X. wrote the paper; A.L. provided financial support; D.L. reviewed the paper; J.Y. proofread the paper. All authors have read and agreed to the published version of the manuscript.

Funding: This research was funded by the National Natural Science Foundation of China (Grant No. 42274013).

Institutional Review Board Statement: Not applicable.

Informed Consent Statement: Not applicable.

Data Availability Statement: Not applicable.

Conflicts of Interest: The authors declare no conflict of interest.

References

1. Li, C.; Long, J.; Huang, M.; Chen, B.; Yang, Y.; Jiang, X.; Xiang, C.; Ma, Z.; He, D.; Chen, L.; et al. Continuous high-precision gravity measurement over 5 months of a Portable Atom Gravimeter in field application. *ESS Open Arch.* **2023**. preprint. [[CrossRef](#)]
2. Chen, X.F.; Hu, D.J.; Zhao, J.; Wu, W.W.; Zhao, H.; Liang, H.; Huang, X.Y. Current status and progress of field experimental observations in the Sichuan region of the China Seismological Science Experimental Range. *Geod. Geodyn.* **2022**, *42*, 193–198.
3. Fu, Z.; Wu, B.; Cheng, B.; Zhou, Y.; Weng, K.; Zhu, D.; Wang, Z.; Lin, Q. A new type of compact gravimeter for long-term absolute gravity monitoring. *Metrologia* **2019**, *56*, 025001. [[CrossRef](#)]
4. Stock, M.; Davis, R.; de Mirandés, E.; Milton, M.J.T. The revision of the SI—The result of three decades of progress in metrology. *Metrologia* **2019**, *56*, 022001. [[CrossRef](#)]
5. Zhu, D.; Zhou, Y.; Wu, B.; Weng, K.; Wang, K.; Cheng, B.; Lin, Q. Metrological traceability method for atomic absolute gravimeters. *Appl. Opt.* **2021**, *60*, 7910–7920. [[CrossRef](#)] [[PubMed](#)]
6. Bassi, A.; Cacciapuoti, L.; Capozziello, S.; Dell’Agnello, S.; Diamanti, E.; Giulini, D.; Iess, L.; Jetzer, P.; Joshi, S.K.; Landragin, A.; et al. A way forward for fundamental physics in space. *NPJ Microgravity* **2022**, *8*, 49. [[CrossRef](#)]
7. Badurina, L.; Buchmueller, O.; Ellis, J.; Lewicki, M.; McCabe, C.; Vaskonen, V. Prospective sensitivities of atom interferometers to gravitational waves and ultralight dark matter. *Philos. Trans. R. Soc. A* **2022**, *380*, 20210060. [[CrossRef](#)] [[PubMed](#)]
8. Tie, J.; Cao, J.; Wu, M.; Lian, J.; Cai, S.; Wang, L. Compensation of Horizontal Gravity Disturbances for High Precision Inertial Navigation. *Sensors* **2018**, *18*, 906. [[CrossRef](#)]

9. Barrett, B.; Antoni-Micollier, L.; Chichet, L.; Battelier, B.; Lévêque, T.; Landragin, A.; Bouyer, P. Dual matter-wave inertial sensors in weightlessness. *Nat. Commun.* **2016**, *7*, 13786. [[CrossRef](#)] [[PubMed](#)]
10. Wang, H.; Wang, K.; Xu, Y.; Tang, Y.; Wu, B.; Cheng, B.; Wu, L.; Zhou, Y.; Weng, K.; Zhu, D.; et al. A Truck-Borne System Based on Cold Atom Gravimeter for Measuring the Absolute Gravity in the Field. *Sensors* **2022**, *22*, 6172. [[CrossRef](#)]
11. Peters, A.; Chung, K.Y.; Chu, S. High-precision gravity measurements using atom interferometry. *Metrologia* **2001**, *38*, 25–61. [[CrossRef](#)]
12. Maxwell, J.C., VIII. A dynamical theory of the electromagnetic field. *Philos. Trans. R. Soc. Lond.* **1865**, *155*, 459–512.
13. Letkhov, V.S.; Minogin, V.G. Trapping and storage of atoms in a laser field. *Appl. Phys.* **1978**, *17*, 99–103. [[CrossRef](#)]
14. Ashkin, A.; Gordon, J.P. Cooling and trapping of atoms by resonance radiation pressure. *Opt. Lett.* **1979**, *4*, 161–163. [[CrossRef](#)] [[PubMed](#)]
15. Dalibard, J.; Reynaud, S.; Cohen-Tannoudji, C. Proposals of stable optical traps for neutral atoms. *Opt. Commun.* **1983**, *47*, 395–399. [[CrossRef](#)]
16. Ashkin, A.; Gordon, J.P. Stability of radiation-pressure particle traps: An optical Earnshaw theorem. *Opt. Lett.* **1983**, *8*, 511–513. [[CrossRef](#)] [[PubMed](#)]
17. Ashkin, A. Stable radiation-pressure particle traps using alternating light beams. *Opt. Lett.* **1984**, *9*, 454. [[CrossRef](#)] [[PubMed](#)]
18. Chu, S.; Bjorkholm, J.E.; Ashkin, A.; Cable, A. Experimental observation of optically trapped atoms. *Phys. Rev. Lett.* **1986**, *57*, 314–317. [[CrossRef](#)] [[PubMed](#)]
19. Pritchard, D.E.; Raab, E.L.; Bagnato, V.; Wieman, C.E.; Watts, R.N. Light Traps Using Spontaneous Forces. *Phys. Rev. Lett.* **1986**, *57*, 310–313. [[CrossRef](#)] [[PubMed](#)]
20. Raab, E.L.; Prentiss, M.; Cable, A.; Chu, S.; Pritchard, D.E. Trapping of Neutral Sodium Atoms with Radiation Pressure. *Phys. Rev. Lett.* **1987**, *59*, 2631–2634. [[CrossRef](#)]
21. Balykin, V.I.; Letokhov, V.S.; Minogin, V.G. Laser Control of the Motion of Neutral Atoms and Optical Atomic Traps. *Phys. Scr.* **1988**, *T22*, 119–127. [[CrossRef](#)]
22. Cohen Tannoudji, C.N.; Phillips, W.D. New Mechanisms for Laser Cooling. *Phys. Today* **1990**, *43*, 33–40. [[CrossRef](#)]
23. Chu, S. Laser Trapping of Neutral Particles. *Sci. Am.-SCI AMER* **1992**, *266*, 71–76. [[CrossRef](#)]
24. Steane, A.M.; Foot, C.J. Laser Cooling below the Doppler Limit in a Magneto-Optical Trap. *Europhys. Lett. (EPL)* **1991**, *14*, 231–236. [[CrossRef](#)]
25. Zhang, D.F.; Gao, T.Y.; Kong, L.R.; Li, K.; Jiang, K.J. Sub-Doppler cooling of rubidium 87 atoms using decompressed magneto-optical trap technique. *J. Quantum Electron.* **2018**, *35*, 308–312.
26. Metcalf, H.J.; van der Straten, P. Laser cooling and trapping of atoms. *J. Opt. Soc. Am. B* **2003**, *20*, 887. [[CrossRef](#)]
27. Gibble, K.E.; Kasapi, S.; Chu, S. Improved magneto-optic trapping in a vapor cell. *Opt. Lett.* **1992**, *17*, 526–528. [[CrossRef](#)] [[PubMed](#)]
28. Steane, A.M.; Chowdhury, M.; Foot, C.J. Radiation force in the magneto-optical trap. *J. Opt. Soc. Am. B* **1992**, *9*, 2142. [[CrossRef](#)]
29. Gabbanini, C.; Evangelista, A.; Gozzini, S.; Lucchesini, A.; Fioretti, A.; Müller, J.H.; Colla, M.; Arimondo, E. Scaling laws in magneto-optical traps. *Europhys. Lett. (EPL)* **1997**, *37*, 251–256. [[CrossRef](#)]
30. Edwards, N.H.; Cooper, C.J.; Zetie, K.P.; Foot, C.J.; Steane, A.M.; Szriftgiser, P.; Perrin, H.; Dalibard, J.; Townsend, C.G. Phase-space density in the magneto-optical trap. *Phys. Rev. A* **1995**, *52*, 1423–1440.
31. Lett, P.D.; Watts, R.N.; Westbrook, C.I.; Phillips, W.D.; Gould, P.L.; Metcalf, H.J. Observation of atoms laser cooled below the Doppler limit. *Phys. Rev. Lett.* **1988**, *61*, 169–172. [[CrossRef](#)] [[PubMed](#)]
32. Wang, X.; Hou, X.K.; Lu, F.F.; Hao, L.L.; He, J.; Wang, J.M. Equivalent temperature measurement of cold atomic samples using a simplified time-of-flight fluorescence imaging method. *J. Quantum Opt.* **2022**, *28*, 223–230.
33. Ketterle, W.; Davis, K.B.; Joffe, M.A.; Martin, A.; Pritchard, D.E. High densities of cold atoms in a dark spontaneous-force optical trap. *Phys. Rev. Lett.* **1993**, *70*, 2253–2256. [[CrossRef](#)] [[PubMed](#)]
34. Walker, T.; Feng, P.; Hoffmann, D.; Williamson, R.S. Spin-polarized spontaneous-force atom trap. *Phys. Rev. Lett.* **1992**, *69*, 2168–2171. [[CrossRef](#)] [[PubMed](#)]
35. Camposo, A.; Piombini, A.; Cervelli, F.; Tantussi, F.; Fuso, F.; Arimondo, E. A cold cesium atomic beam produced out of a pyramidal funnel. *Opt. Commun.* **2001**, *200*, 231–239. [[CrossRef](#)]
36. Bowden, W.; Hobson, R.; Hill, I.R.; Vianello, A.; Schioppo, M.; Silva, A.; Margolis, H.S.; Baird, P.; Gill, P. A pyramid MOT with integrated optical cavities as a cold atom platform for an optical lattice clock. *Sci. Rep.* **2019**, *9*, 11704. [[CrossRef](#)] [[PubMed](#)]
37. Kim, J.A.; Lee, K.I.; Noh, H.R.; Jhe, W.; Ohtsu, M. Atom trap in an axicon mirror. *Opt. Lett.* **1997**, *22*, 117. [[CrossRef](#)] [[PubMed](#)]
38. Lee, K.I.; Kim, J.A.; Noh, H.R.; Jhe, W. Single-beam atom trap in a pyramidal and conical hollow mirror. *Opt. Lett.* **1996**, *21*, 1177. [[CrossRef](#)] [[PubMed](#)]
39. Bhushan, S.; Easwaran, R.K. Theoretical design for generation of slow light in a two-dimensional magneto optical trap using electromagnetically induced transparency. *Appl. Opt.* **2017**, *56*, 3817–3823. [[CrossRef](#)] [[PubMed](#)]
40. Hummon, M.T.; Yeo, M.; Stuhl, B.K.; Collopy, A.L.; Xia, Y.; Ye, J. 2D Magneto-optical trapping of diatomic molecules. *Phys. Rev. Lett.* **2013**, *110*, 143001. [[CrossRef](#)] [[PubMed](#)]
41. Ramirez-Serrano, J.; Yu, N.; Kohel, J.M.; Kellogg, J.R.; Maleki, L. Multistage two-dimensional magneto-optical trap as a compact cold atom beam source. *Opt. Lett.* **2006**, *31*, 682–684. [[CrossRef](#)] [[PubMed](#)]

42. Yun, M.; Yin, J. Practical scheme to realize 2D array of BECs on an atom chip: Novel 2D magneto-optical and magnetic lattices. *Opt. Express* **2006**, *14*, 2539–2551. [[CrossRef](#)] [[PubMed](#)]
43. Zhang, S.; Chen, J.F.; Liu, C.; Zhou, S.; Loy, M.M.; Wong, G.K.; Du, S. A dark-line two-dimensional magneto-optical trap of 85Rb atoms with high optical depth. *Rev. Sci. Instrum.* **2012**, *83*, 073102. [[CrossRef](#)] [[PubMed](#)]
44. Barry, J.F.; McCarron, D.J.; Norrgard, E.B.; Steinecker, M.H.; DeMille, D. Magneto-optical trapping of a diatomic molecule. *Nature* **2014**, *512*, 286–289. [[CrossRef](#)] [[PubMed](#)]
45. Monroe, C.; Swann, W.; Robinson, H.; Wieman, C. Very cold trapped atoms in a vapor cell. *Phys. Rev. Lett.* **1990**, *65*, 1571–1574. [[CrossRef](#)]
46. Freier, C.; Hauth, M.; Schkolnik, V.; Leykauf, B.; Schilling, M.; Wziontek, H.; Scherneck, H.; Müller, J.; Peters, A. Mobile quantum gravity sensor with unprecedented stability. *J. Phys. Conf. Ser.* **2016**, *723*, 012050. [[CrossRef](#)]
47. Hauth, M.; Freier, C.; Schkolnik, V.; Senger, A.; Schmidt, M.; Peters, A. First gravity measurements using the mobile atom interferometer GAIN. *Appl. Phys. B* **2013**, *113*, 49–55. [[CrossRef](#)]
48. Bidet, Y.; Zahzam, N.; Blanchard, C.; Bonnin, A.; Cadoret, M.; Bresson, A.; Rouxel, D.; Lequentrec-Lalancette, M.F. Absolute marine gravimetry with matter-wave interferometry. *Nat. Commun.* **2018**, *9*, 6172. [[CrossRef](#)]
49. Bidet, Y.; Zahzam, N.; Bresson, A.; Blanchard, C.; Cadoret, M.; Olesen, A.V.; Forsberg, R. Absolute airborne gravimetry with a cold atom sensor. *Geodesy* **2020**, *94*, 1–9. [[CrossRef](#)]
50. Li, Z.Y.; Hu, M.Z.; Wang, Y.; Liu, Z.W.; Wu, Y.L.; Zhang, X.L.; Wang, J.P.; Wang, J.; Li, F. Field test results of a domestic rubidium atomic absolute gravimeter. *Proc. Chin. Jt. Annu. Geosci. Conf.* **2021**, *29*, 1.
51. Shimizu, F.; Shimizu, K.; Takuma, H. Laser cooling and trapping of Ne metastable atoms. *Phys. Rev. A* **1989**, *39*, 2758–2760. [[CrossRef](#)] [[PubMed](#)]
52. Shimizu, F.; Shimizu, K.; Takuma, H. Four-beam laser trap of neutral atoms. *Opt. Lett.* **1991**, *16*, 339. [[CrossRef](#)]
53. Arlt, J.; Bance, P.; Hopkins, S.; Martin, J.; Webster, S.; Wilson, A.; Zetie, K.; Foot, C.J. Suppression of collisional loss from a magnetic trap. *J. Phys. B At. Mol. Opt. Phys.* **1998**, *31*, L321–L327. [[CrossRef](#)]
54. di Stefano, A.; Wilkowski, D.; Müller, J.H.; Arimondo, E. Five-beam magneto-optical trap and optical molasses. *Appl. Phys. B* **1999**, *69*, 263–268. [[CrossRef](#)]
55. Zhou, Y.; Zhang, C.; Chen, P.; Cheng, B.; Zhu, D.; Wang, K.; Wang, X.; Wu, B.; Qiao, Z.; Lin, Q.; et al. A Testing Method for Shipborne Atomic Gravimeter Based on the Modulated Coriolis Effect. *Sensors* **2023**, *23*, 881. [[CrossRef](#)] [[PubMed](#)]
56. Che, H.; Li, A.; Fang, J.; Ge, G.; Gao, W.; Zhang, Y.; Liu, C.; Xu, J.N.; Chang, L.B.; Huang, C.F.; et al. Experimental study on shipboard dynamic absolute gravity measurement based on cold atomic gravimeter. *J. Phys.* **2022**, *71*, 148–156.
57. Geiger, R.; Ménot, V.; Stern, G.; Zahzam, N.; Cheinet, P.; Battelier, B.; Villing, A.; Moron, F.; Lours, M.; Bidet, Y.; et al. Detecting inertial effects with airborne matter-wave interferometry. *Nat. Commun.* **2011**, *2*, 474. [[CrossRef](#)]
58. Wu, B.; Zhou, Y.; Cheng, B.; Zhu, D.; Wang, K.N.; Zhu, X.X.; Chen, P.J.; Weng, K.X.; Yang, Q.H.; Lin, J.H.; et al. Vehicle-mounted static absolute gravity measurements based on an atomic gravimeter. *J. Phys.* **2020**, *69*, 25–32.
59. Cheng, B.; Chen, P.J.; Zhou, Y.; Wang, K.N.; Zhu, D.; Chu, L.; Weng, K.X.; Wang, H.L.; Peng, S.P.; Wang, X.L.; et al. Absolute gravity dynamical mobility measurement experiment based on cold atomic gravimeter. *J. Phys.* **2022**, *71*, 247–257.
60. Zhang, X.; Zhong, J.; Tang, B.; Chen, X.; Zhu, L.; Huang, P.; Wang, J.; Zhan, M. Compact portable laser system for mobile cold atom gravimeters. *Appl. Opt.* **2018**, *57*, 6545–6551. [[CrossRef](#)] [[PubMed](#)]
61. Luo, Q.; Zhang, H.; Zhang, K.; Duan, X.C.; Hu, Z.K.; Chen, L.L.; Zhou, M.K. A compact laser system for a portable atom interferometry gravimeter. *Rev. Sci. Instrum.* **2019**, *90*, 043104. [[CrossRef](#)] [[PubMed](#)]
62. Fang, J.; Hu, J.; Chen, X.; Zhu, H.; Zhou, L.; Zhong, J.; Wang, J.; Zhan, M. Realization of a compact one-seed laser system for atom interferometer-based gravimeters. *Opt. Express* **2018**, *26*, 1586–1596. [[CrossRef](#)] [[PubMed](#)]
63. Sabulsky, D.O.; Junca, J.; Lefèvre, G.; Zou, X.; Bertoldi, A.; Battelier, B.; Prevedelli, M.; Stern, G.; Santoire, J.; Beaufiles, Q.; et al. A fibered laser system for the MIGA large scale atom interferometer. *Sci. Rep.* **2020**, *10*, 3268. [[CrossRef](#)] [[PubMed](#)]
64. Xu, R.; Wang, Q.; Yan, S.; Hou, Z.; He, C.; Ji, Y.; Li, Z.; Jiang, J.; Qiao, B.; Zhou, L.; et al. Modular-assembled laser system for a long-baseline atom interferometer. *Appl. Opt.* **2022**, *61*, 4648–4654. [[CrossRef](#)] [[PubMed](#)]
65. Adams, C.S.; Riis, E. Laser cooling and trapping of neutral atoms. *Prog. Quant. Electron.* **1997**, *21*, 1–79. [[CrossRef](#)]
66. Lu, Z.T.; Corwin, K.L.; Renn, M.J.; Anderson, M.H.; Cornell, E.A.; Wieman, C.E. Low-Velocity Intense Source of Atoms from a Magneto-optical Trap. *Phys. Rev. Lett.* **1996**, *77*, 3331–3334. [[CrossRef](#)] [[PubMed](#)]
67. Williamson, R.; Voytas, P.; Newell, R.; Walker, T. A magneto-optical trap loaded from a pyramidal funnel. *Opt. Express* **1998**, *3*, 111–117. [[CrossRef](#)]
68. Arlt, J.J.; Maragò, O.; Webster, S.; Hopkins, S.; Foot, C.J. A pyramidal magneto-optical trap as a source of slow atoms. *Opt. Commun.* **1998**, *157*, 303–309. [[CrossRef](#)]
69. Kohel, J.M.; Ramirez-Serrano, J.; Thompson, R.J.; Maleki, L.; Bliss, J.L.; Libbrecht, K.G. Generation of an intense cold-atom beam from a pyramidal magneto-optical trap: Experiment and simulation. *J. Opt. Soc. Am. B* **2003**, *20*, 1161. [[CrossRef](#)]
70. Bodart, Q.; Merlet, S.; Malossi, N.; Dos Santos, F.P.; Bouyer, P.; Landragin, A. A cold atom pyramidal gravimeter with a single laser beam. *Appl. Phys. Lett.* **2010**, *96*, 134101. [[CrossRef](#)]
71. Kasevich, M.; Weiss, D.S.; Riis, E.; Moler, K.; Kasapi, S.; Chu, S. Atomic velocity selection using stimulated Raman transitions. *Phys. Rev. Lett.* **1991**, *66*, 2297–2300. [[CrossRef](#)] [[PubMed](#)]

72. Lautier, J.; Landragin, A.; Battelier, B.; Bouyer, P. *MiniAtom: Realization of an Absolute Compact Atomic Gravimeter*; IEEE: New York, NY, USA, 2013; pp. 448–449.
73. Louchet-Chauvet, A.; Farah, T.; Bodart, Q.; Clairon, A.; Landragin, A.; Merlet, S.; Santos, F.P.D. The influence of transverse motion within an atomic gravimeter. *New J. Phys.* **2011**, *13*, 065025. [[CrossRef](#)]
74. Ménoret, V.; Vermeulen, P.; Le Moigne, N.; Bonvalot, S.; Bouyer, P.; Landragin, A.; Desruelle, B. Gravity measurements below 10–9 g with a transportable absolute quantum gravimeter. *Sci. Rep.* **2018**, *8*, 12300. [[CrossRef](#)] [[PubMed](#)]
75. Wu, X.; Weiner, S.; Pagel, Z.; Malek, B.S.; Muller, H. Mobile Quantum Gravimeter with a Novel Pyramidal Magneto-Optical Trap. In Proceedings of the CLEO, Washington, DC, USA, 10–15 May 2020; pp. 1–2.
76. Wu, X.; Pagel, Z.; Malek, B.S.; Nguyen, T.H.; Zi, F.; Scheirer, D.S.; Muller, H. Gravity surveys using a mobile atom interferometer. *Sci. Adv.* **2019**, *5*, eaax0800. [[CrossRef](#)] [[PubMed](#)]
77. Wu, X.; Zi, F.; Dudley, J.; Bilotta, R.J.; Canoza, P.; Müller, H. Multiaxis atom interferometry with a single-diode laser and a pyramidal magneto-optical trap. *Optica* **2017**, *4*, 1545. [[CrossRef](#)]
78. Dieckmann, K.; Spreew, R.J.C.; Weidemüller, M.; Walraven, J.T.M. Two-dimensional magneto-optical trap as a source of slow atoms. *Phys. Rev. A* **1998**, *58*, 3891–3895. [[CrossRef](#)]
79. Zeng, D.J.; Huang, M.; Zhang, H.; Huang, K.K.; Lu, X.H. A two-dimensional cold atomic beam system for increasing the loading rate of three-dimensional magneto-optical traps. *Infrared Laser Eng.* **2019**, *48*, 73–78.
80. Wang, K.N.; Xu, H.; Zhou, Y.; Xu, Y.P.; Song, W.; Tang, H.Z.; Wang, Q.W.; Zhu, D.; Weng, K.X.; Wang, H.L.; et al. Rapid mapping of absolute gravity in the external field based on a vehicle-mounted atomic gravimeter. *J. Phys.* **2022**, *71*, 347–356.
81. Jin, S.; Gao, J.; Chandrashekhara, K.; Götzhäuser, C.; Schöner, J.; Chomaz, L. A 2D MOT of dysprosium atoms as a compact source for efficient loading of a narrow-line 3D MOT. *arXiv* **2023**, arXiv:2303.05191.
82. Zhang, Y.; Liu, Q.; Sun, J.; Xu, Z.; Wang, A. Enhanced cold mercury atom production with two-dimensional magneto-optical trap. *Chin. Phys. B* **2022**, *31*, 073701. [[CrossRef](#)]
83. Eriksson, S.; Trupke, M.; Powell, H.F.; Sahagun, D.; Sinclair, C.D.J.; Curtis, E.A.; Sauer, B.E.; Hinds, E.A.; Muktadir, Z.; Gollasch, C.O.; et al. Integrated optical components on atom chips. *Eur. Phys. J. D* **2005**, *35*, 135–139. [[CrossRef](#)]
84. Trupke, M.; Ramirez-Martinez, F.; Curtis, E.A.; Ashmore, J.P.; Eriksson, S.; Hinds, E.A.; Muktadir, Z.; Gollasch, C.; Kraft, M.; Vijaya Prakash, G.; et al. Pyramidal micromirrors for microsystems and atom chips. *Appl. Phys. Lett.* **2006**, *88*, 071116. [[CrossRef](#)]
85. Blumenthal, D.J. Photonic integration for UV to IR applications. *APL Photonics* **2020**, *5*, 020903. [[CrossRef](#)]
86. Pollock, S.; Cotter, J.P.; Lalot, A.; Hinds, E.A. Integrated magneto-optical traps on a chip. *Opt. Express* **2009**, *17*, 14109. [[CrossRef](#)] [[PubMed](#)]
87. Lewis, G.N.; Muktadir, Z.; Gollasch, C.; Kraft, M.; Pollock, S.; Ramirez-Martinez, F.; Ashmore, J.P.; Lalot, A.; Trupke, M.; Hinds, E.A. Fabrication of Magneto-optical Atom Traps on a Chip. *J. Microelectromech. Syst.* **2009**, *18*, 347–353. [[CrossRef](#)]
88. Vangeleyn, M.; Griffin, P.F.; Riis, E.; Arnold, A.S. Single-laser, one beam, tetrahedral magneto-optical trap. *Opt. Express* **2009**, *17*, 13601–13608. [[CrossRef](#)]
89. Lee, J.; Grover, J.A.; Orozco, L.A.; Rolston, S.L. Sub-Doppler cooling of neutral atoms in a grating magneto-optical trap. *J. Opt. Soc. Am. B* **2013**, *30*, 2869. [[CrossRef](#)]
90. McGilligan, J.P.; Griffin, P.F.; Elvin, R.; Ingleby, S.J.; Riis, E.; Arnold, A.S. Grating chips for quantum technologies. *Sci. Rep.* **2017**, *7*, 387. [[CrossRef](#)]
91. Barker, D.S.; Norrgard, E.B.; Klimov, N.N.; Fedchak, J.A.; Scherschligt, J.; Eckel, S. Single-beam Zeeman slower and magneto-optical trap using a nanofabricated grating. *Phys. Rev. Appl.* **2019**, *11*, 064023. [[CrossRef](#)]
92. McGehee, W.R.; Zhu, W.; Barker, D.S.; Westly, D.; Yulaev, A.; Klimov, N.; Agrawal, A.; Eckel, S.; Aksyuk, V.; McClelland, J.J. Magneto-optical trapping using planar optics. *New J. Phys.* **2021**, *23*, 013021. [[CrossRef](#)]
93. Earl, L.; Vovrosh, J.; Wright, M.; Roberts, D.; Winch, J.; Perea-Ortiz, M.; Lamb, A.; Hayati, F.; Griffin, P.; Metje, N.; et al. Demonstration of a Compact Magneto-Optical Trap on an Unstaffed Aerial Vehicle. *Atoms* **2022**, *10*, 32. [[CrossRef](#)]
94. Lee, J.; Ding, R.; Christensen, J.; Rosenthal, R.R.; Ison, A.; Gillund, D.P.; Bossert, D.; Fuerschbach, K.H.; Kindel, W.; Finnegan, P.S.; et al. A compact cold-atom interferometer with a high data-rate grating magneto-optical trap and a photonic-integrated-circuit-compatible laser system. *Nat. Commun.* **2022**, *13*, 5131. [[CrossRef](#)] [[PubMed](#)]
95. Duan, J.; Liu, X.; Zhou, Y.; Xu, X.; Chen, L.; Zou, C.; Zhu, Z.; Yu, Z.; Ru, N.; Qu, J. High diffraction efficiency grating atom chip for magneto-optical trap. *Opt. Commun.* **2022**, *513*, 128087. [[CrossRef](#)]
96. Huang, C.; Xu, X.; Zhang, Y.; Ma, D.; Lu, Z.; Wang, Z.; Chen, G.; Zhang, J.; Tang, H.X.; Dong, C.; et al. Planar-Integrated Magneto-Optical Trap. *Phys. Rev. Appl.* **2022**, *17*, 034031.
97. Burrow, O.S.; Osborn, P.F.; Boughton, E.; Mirando, F.; Burt, D.P.; Griffin, P.F.; Arnold, A.S.; Riis, E. Stand-alone vacuum cell for compact ultracold quantum technologies. *Appl. Phys. Lett.* **2021**, *119*, 124002. [[CrossRef](#)]
98. Trimeche, A.; Battelier, B.; Becker, D.; Bertoldi, A.; Bouyer, P.; Braxmaier, C.; Charron, E.; Corgier, R.; Cornelius, M.; Douch, K.; et al. Concept study and preliminary design of a cold atom interferometer for space gravity gradiometry. *Class. Quant Grav* **2019**, *36*, 215004. [[CrossRef](#)]
99. Loriani, S.; Schlippert, D.; Schubert, C.; Abend, S.; Ahlers, H.; Ertmer, W.; Rudolph, J.; Hogan, J.M.; Kasevich, M.A.; Rasel, E.M.; et al. Atomic source selection in space-borne gravitational wave detection. *New J. Phys.* **2019**, *21*, 63030. [[CrossRef](#)]

100. Nshii, C.C.; Vangeleyn, M.; Cotter, J.P.; Griffin, P.F.; Hinds, E.A.; Ironside, C.N.; See, P.; Sinclair, A.G.; Riis, E.; Arnold, A.S. A surface-patterned chip as a strong source of ultracold atoms for quantum technologies. *Nat. Nanotechnol.* **2013**, *8*, 321–324. [[CrossRef](#)]
101. Elvin, R.; Hoth, G.W.; Wright, M.; Lewis, B.; McGilligan, J.P.; Arnold, A.S.; Griffin, P.F.; Riis, E. Cold-atom clock based on a diffractive optic. *Opt. Express* **2019**, *27*, 38359. [[CrossRef](#)]
102. Franssen, J.G.H.; de Raadt, T.C.H.; van Nindhuis, M.A.W.; Luiten, O.J. Compact ultracold electron source based on a grating magneto-optical trap. *Phys. Rev. Accel. Beams* **2019**, *22*, 023401. [[CrossRef](#)]
103. Eckel, S.; Barker, D.S.; Fedchak, J.A.; Klimov, N.N.; Norrgard, E.; Scherschligt, J.; Makrides, C.; Tiesinga, E. Challenges to miniaturizing cold atom technology for deployable vacuum metrology. *Metrologia* **2018**, *55*, S182–S193. [[CrossRef](#)]
104. Bondza, S.; Lisdat, C.; Kroker, S.; Leopold, T. Two-Color Grating Magneto-Optical Trap for Narrow-Line Laser Cooling. *Phys. Rev. Appl.* **2022**, *17*, 044002. [[CrossRef](#)]
105. Imhof, E.; Stuhl, B.K.; Kasch, B.; Kroese, B.; Olson, S.E.; Squires, M.B. Two-dimensional grating magneto-optical trap. *Phys. Rev. A* **2017**, *96*, 033636. [[CrossRef](#)]
106. Sitaram, A.; Elgee, P.K.; Campbell, G.K.; Klimov, N.N.; Eckel, S.; Barker, D.S. Confinement of an alkaline-earth element in a grating magneto-optical trap. *Rev. Sci. Instrum.* **2020**, *91*, 103202. [[CrossRef](#)] [[PubMed](#)]
107. Rushton, J.A.; Aldous, M.; Himsworth, M.D. Contributed Review: The feasibility of a fully miniaturized magneto-optical trap for portable ultracold quantum technology. *Rev. Sci. Instrum.* **2014**, *85*, 121501. [[CrossRef](#)] [[PubMed](#)]
108. Keil, M.; Amit, O.; Zhou, S.; Groswasser, D.; Japha, Y.; Folman, R. Fifteen years of cold matter on the atom chip: Promise, realizations, and prospects. *J. Mod. Opt.* **2016**, *63*, 1840–1885. [[CrossRef](#)] [[PubMed](#)]
109. Birkel, G.; Buchkremer, F.B.J.; Dumke, R.; Ertmer, W. Atom optics with microfabricated optical elements. *Opt. Commun.* **2001**, *191*, 67–81. [[CrossRef](#)]

Disclaimer/Publisher's Note: The statements, opinions and data contained in all publications are solely those of the individual author(s) and contributor(s) and not of MDPI and/or the editor(s). MDPI and/or the editor(s) disclaim responsibility for any injury to people or property resulting from any ideas, methods, instructions or products referred to in the content.